(2)

GLUCOSE ELECTRODES BASED ON CROSS-LINKED $[Os(bpy)_2Cl]^{+/2+}$ COMPLEXED POLY(1-VINYLIMIDAZOLE) FILMS

Timothy J. Ohara and Adam Heller
Department of Chemical Engineering
University of Texas at Austin
Austin, TX 78712-1062

sent to Anal. Chem. 4/21/93

Abstract

Enzyme electrodes based on a redox hydrogel formed upon complexing water-soluble poly(1-vinylimidazole) ("PVI") with $[Os(bpy)_2Cl]^+$ ("Os") and cross-linked with water-soluble poly(ethylene glycol) diglycidyl ether (molecular weight 400, peg 400) are described. The properties of the electrodes depended on their polymers' osmium content, its extent of cross-linking, on the pH, and the ionic strength in which they were used. The redox hydrogels' electron diffusion coefficients (D_e) increased with osmium content of their polymers. The D_e values were 1.5×10^{-8} cm^2 s^{-1}, 1.3×10^{-8} cm^2 s^{-1}, 4.3×10^{-9} cm^2 s^{-1} for PVI_3-Os, PVI_5-Os, and PVI_{10}-Os, respectively, the subscripts indicating the number of monomer units per osmium redox center. D_e decreased with increasing ionic strength and increased upon protonation of the polymer. In glucose electrodes, made by incorporating in the films glucose oxidase (GOX) through covalent bonding in the cross-linking step, glucose was electrooxidized at 250 mV (SCE). The characteristics of these electrodes depended on the GOX concentration, film thickness, O_2 concentration, pH, NaCl concentration, and electrode potential. The steady-state glucose electrooxidation currents were independent of the polymers' osmium content in the studied (3 - 10 osmium centers per monomer unit) range. Electrodes containing 39% GOX reached

30pp

UNCLASSIFIED

SECURITY CLASSIFICATION OF THIS PAGE

REPORT DOCUMENTATION PAGE

Form Approved OMB No. 0704-0188

1a. REPORT SECURITY CLASSIFICATION UNCLASSIFIED	1b RESTRICTIVE MARKINGS NONE
2a. SECURITY CLASSIFICATION AUTHORITY	3 DISTRIBUTION/AVAILABILITY OF REPORT APPROVED FOR PUBLIC RELEASE AND SALE: its distribution is unlimited
2b. DECLASSIFICATION/DOWNGRADING SCHEDULE	
4. PERFORMING ORGANIZATION REPORT NUMBER(S) TECHNICAL REPORT NO. 005	5. MONITORING ORGANIZATION REPORT NUMBER(S)
6a. NAME OF PERFORMING ORGANIZATION UNIVERSITY OF TEXAS AT AUSTIN 6b. OFFICE SYMBOL (If applicable)	7a. NAME OF MONITORING ORGANIZATION DEPARTMENT OF SPONSORED PROJECTS THE UNIVERSITY OF TEXAS AT AUSTIN
6c. ADDRESS (City, State, and ZIP Code) Department of Chemical Engineering Austin, TX 78712-1062	7b. ADDRESS (City, State, and ZIP Code) P.O. Box 7726 Austin, TX 78713-7726
8a. NAME OF FUNDING/SPONSORING ORGANIZATION OFFICE OF NAVAL RESEARCH 8b. OFFICE SYMBOL (If applicable)	9. PROCUREMENT INSTRUMENT IDENTIFICATION NUMBER
8c. ADDRESS (City, State, and ZIP Code) 800 N. Quincy Street Arlington, VA 22217	10. SOURCE OF FUNDING NUMBERS PROGRAM ELEMENT NO. / PROJECT NO. / TASK NO / WORK UNIT ACCESSION NO.

11. TITLE (Include Security Classification) Glucose Electrodes based on Crosslinked $[Os(bpy)_2Cl]^{+/2+}$ Complexed Poly(1-Vinylimidazole) Films
UNCLASSIFIED

12. PERSONAL AUTHOR(S)
T.J. Ohara and Adam Heller

13a. TYPE OF REPORT	13b. TIME COVERED	14. DATE OF REPORT (Year, Month, Day)	15. PAGE COUNT
TECHNICAL	FROM 10/92 TO 5/93	1993 May 24	2

16. SUPPLEMENTARY NOTATION

17. COSATI CODES			18. SUBJECT TERMS (Continue on reverse if necessary and identify by block number)
FIELD	GROUP	SUB-GROUP	Glucose; Electrodes; Hydrogel; Poly(1-vinylimidazole

19. ABSTRACT (Continue on reverse if necessary and identify by block number)

Enzyme electrodes based on a redox hydrogel formed upon complexing water-soluble poly(1-vinylimidazole) ("PVI") with $[Os(bpy)_2Cl]^+$ ("Os") and cross-linked with water-soluble poly(ethylene glycol) diglycidyl ether (molecular weight 400, peg 400) are described. The properties of the electrodes depended on their polymers' osmium content, its extent of cross-linking, on the pH, and the ionic strength in which they were used. The redox hydrogels' electron diffusion coefficients (D_e) increased with osmium content of their polymers. The D_e values were 1.5 X 10^{-8} cm^2 s^{-1}, 1.3 X 10^{-8} cm^2 s^{-1}, 4.3 X

(Continued)

20. DISTRIBUTION/AVAILABILITY OF ABSTRACT	21. ABSTRACT SECURITY CLASSIFICATION
☒ UNCLASSIFIED/UNLIMITED ☐ SAME AS RPT ☐ DTIC USERS	UNCLASSIFIED
22a. NAME OF RESPONSIBLE INDIVIDUAL Adam Heller	22b TELEPHONE (Include Area Code) (512) 471-8874 / 22c OFFICE SYMBOL

DD Form 1473, JUN 86 Previous editions are obsolete. SECURITY CLASSIFICATION OF THIS PAGE
UNCLASSIFIED

(CONTINUED: BLOCK 19):

10^{-9} cm^2 s^{-1} for PVI_3-Os, PVI_5-Os, and PVI_{10}-Os, respectively, the subscripts indicating the number of monomer units per osmium redox center. D_e decreased with increasing ionic strength and increased upon protonation of the polymer. In glucose electrodes, made by incorporating in the films glucose oxidase (GOX) through covalent bonding in the cross-linking step, glucose was electrooxidized at 250 mV (SCE). The characteristics of these electrodes depended on the GOX concentration, film thickness, O_2 concentration, pH, NaCl concentration, and electrode potential. The steady-state glucose electrooxidation currents were independent of the polymers' osmium content in the studied (3 - 10 osmium centers per monomer unit) range. Electrodes containing 39% GOX reached steady-state glucose electrooxidation current densities of 400 μa cm^{-2} and, when made with thick gel films, were selective for glucose in the presence of physiological concentrations of ascorbate and acetaminophen.

steady-state glucose electrooxidation current densities of 400 μa cm^{-2} and, when made with thick gel films, were selective for glucose in the presence of physiological concentrations of ascorbate and acetaminophen.

Introduction

Redox hydrogel films are unique in having both adequate electron diffusion coefficients and in being permeable to water soluble substrates and products of enzymatic reactions.[1] When a cross-linked redox polymer network electrically "wires" an enzyme that is covalently bound to it, then the gel and the current collecting metal form enzyme electrodes. Such electrodes are potentially useful in applications where release of diffusional mediators from the electrodes is to be avoided and where small size is important.[2] Here we show that hydrogels, based on the Os complex of PVI are adequate electron conductors and that glucose oxidase (GOX) transfers electrons through the gel's polymer network to electrodes. The hydrogels are made by cross-linking with poly(ethylene glycol) diglycidyl ether (peg 400), PVI_n-Os, and GOX.

A reference polymer with which the PVI_n-Os polymers is compared is poly(4-vinylpyridine) ("PVP") complexed with osmium ("POs") and partially quaternized with bromoethylamine ("POs-EA").[3] POs is only marginally soluble in water except at high osmium loading. POs-EA is, however, water soluble and easy to cross-link with diepoxides such as peg 400 that binds POs-EA amines and lysyl functions of enzyme proteins.[4] The resulting redox hydrogel adheres well to the electrodes. In contrast with the PVP derived polymers, the PVI_n-Os polymers are highly water soluble and do not require quaternization with bromoethylamine for easy cross-linking with water-soluble diepoxides. The redox potential of PVI_n-Os is 200 mV (SCE) vs 280 mV (SCE) for POs or POs-EA.

Because the operating potentials of the resulting enzyme electrodes is also lower, currents resulting from electrooxidation of some interferants are reduced.

Experimental Section

Chemicals. 1-vinylimidazole (Aldrich), K_2OsCl_6 (Johnson Matthey), 2,2'-bipyridine (Aldrich), Na-HEPES (sodium 4-(2-hydroxyethyl)-1-piperazineethanesulfonate) (Aldrich), poly(ethylene glycol) diglycidyl ether (Polysciences, peg 400, cat. no. 08210), and glucose oxidase (EC 1.1.3.4) from Aspergillus niger (type X-S, 198 units) were used as received. 2,2'-azo-bis(isobutyronitrile) (Polysciences, AIBN) was purified by double recrystallization from methanol and stored at -20°C. $Os(bpy)_2Cl_2$ was prepared by a reported procedure.[5]

Poly(1-vinylimidazole), (PVI). Bulk polymerization of PVI was carried out by heating 6 ml of 1-vinylimidazole and 0.5 g of AIBN at 70°C for 2 hours under Ar. A dark yellow precipitate formed soon after heating. After allowing the reaction mixture to cool, the precipitate was dissolved in methanol and added dropwise to a strongly stirred solution of acetone. The filtered precipitate was a pale yellow hygroscopic solid. The molecular weight of the polymer was found, by HPLC analysis using a Synchrom Catsec 300 column with 0.1% trifluoroacetic acid and 0.2 M NaCl as the elutant, to be about 7000 g mol^{-1}. The flow rate in the molecular weight determination was 0.4 ml/min and poly(2-vinylpyridine) was used as the standard.

PVI_n-Os, n = 3, 5, 10. Osmium derivatized polymers were prepared by a procedure similar to that of Forster and Vos[6] where the appropriate amount of $Os(bpy)_2Cl_2$ was refluxed with PVI in ethanol for 3 days. The elemental analyses were: Calculated for $C_{35}Cl_2H_{34}N_{10}Os \cdot 3\ H_2O$: C, 46.2; H, 4.4; N, 15.4; Os, 20.9; Found C, 46.4; H, 4.2; N, 15.3; Os, 18.4. Calculated for

$C_{45}Cl_2H_{46}N_{14}Os \cdot 5\ H_2O$: C, 47.7; H, 5.0; N, 17.3; Os, 16.8; Found C, 48.2; H, 4.5; N, 16.2; Os, 15.4. Calculated for $C_{70}Cl_2H_{76}N_{24}Os \cdot 10\ H_2O$: C, 49.6; H, 5.7; N, 19.9; Os, 11.2; Found C, 51.1; H, 5.2; N, 18.7; Os, 11.0. The three osmium derivatized polymers are referred to as PVI_3-Os, PVI_5-Os, and PVI_{10}-Os where the subscript represents the number of vinylimidazole units per $Os(bpy)_2Cl$.

Electrodes. Rotating disk electrodes were prepared by embedding vitreous carbon rods (3 mm diameter, V-10, Atomergic) in a teflon shroud using a low viscosity epoxy (Polysciences, cat. no. 01916). Electrodes were prepared by syringing a 2 μl aliquot of 5 mg ml $^{-1}$ PVI_n-Os solution onto the electrode surface (0.071 cm^2). Next, a 2 μl volume of a 4 mg ml $^{-1}$ (10 mM HEPES pH = 8.1) solution of glucose oxidase was added on the electrode and stirred with a syringe needle. In the final step, 1.2 μl of a 2.5 mg/ml solution of peg 400 was added to the electrode and stirred. The electrode was allowed to cure for at least 48 hours under vacuum.

Measurements. Electrochemical measurements were performed with a Princeton Applied Research 175 universal programmer, a Model 173 potentiostat and a Model 179 digital coulometer. The signal was recorded on a Kipp and Zonen X-Y-Y' recorder. Rotating disk electrode experiments were performed with a Pine Instruments AFMSRX rotator with an MSRS speed controller. The three -electrode cell contained 0.1 M NaCl buffered with phosphate (20 mM, pH = 7.2). The current response of the glucose electrodes were found to have a sigmoidal dependence on potential resulting in a maximum oxidation current at potentials $\geq$300 mV (SCE). In the constant potential experiments, the working electrode was poised at 0.4 V (SCE) to ensure that the maximum oxidation current to glucose was observed. The chronoamperometric measurements were performed with a Princeton Applied Research Model 273 potentiostat. The

potential was initially held at 0.0 V (SCE) for 15 s, then stepped to 0.8 V for 0.3 s. The slopes of the resulting i vs $t^{-1/2}$ plots were unaffected upon varying the residence time (0.1 to 0.5 s). Three hundred data points were recorded. The reported values are averages of either four or five measurements.

Results and Discussion

Cyclic Voltammetry of PVI_n-Os-Peg 400 Coated Electrodes.

The effect of the extent of cross-linking on the electrochemical behavior of PVI_n-Os (n = 3, 5, 10) films cross-linked with 5% to 20% peg 400 was determined for electrodes in which the quantity of redox polymer was held constant, with the films cured for > 48 hours. Coulometry (by cyclic voltammetry) showed that appproximately 50% of the osmium was immobilized and that it did not vary with the extent of cross-linking. The cross-linked films adhered well to the vitreous carbon electrodes and retained about 95% of their electroactive osmium when soaked in a stirred phosphate buffer at room temperature for 72 hours.

The separation of the oxidation and the reduction peaks (ΔE_p) of the voltammograms at 100 mV s^{-1} scan rate remained constant at ~ 100 mV through the cross-linking range studied. In contrast to POs-EA films, ΔE_p increased with the cross-linker (peg 400) concentrations.[3]

The peak width at half-height (E_{fwhm}) (for the oxidation wave measured at 1 mV s^{-1}) increased with the extent of cross-linking from 60 mV to 110 mV for PVI_n-Os (n = 3, 5, 10). While in the POs-EA system the E_{fwhm} of the oxidation peak was narrower than that of the reduction peak, in the PVI_n-Os-peg 400 systems the two were precisely equal.[3]

Diffusion Coefficients. $D_eC_p^2$ values (D_e being the electron diffusion coefficient and C_p the concentration of the redox couple in the film) were measured for the cross-linked films by potential step chronoamperometry.[7] The

film thickness was calculated by assuming that all three osmium polymers had a density of 1 g cm^{-3}. There was no discernible trend in the dependence of $D_eC_p^2$ on cross-linking (Table 1). D_e was, however, higher in the PVI_5-Os polymer films than in the cross-linked POs-EA films by a factor of five.[3] D_e was higher and nearly identical for PVI_3-Os and PVI_5-Os films, and lower for PVI_{10}-Os films.

Effects of Ionic Strength and pH on the Electron Diffusion Coefficients. As seen in Figure 1, $D_eC_p^2$ decreased with increasing NaCl concentration through the 88 mM to 2000 mM range. Specifically, $D_eC_p^2$ decreased by about 50% when the NaCl concentration was raised from 88 mM to 1000 mM NaCl.

Figure 2 shows the pH dependence of $D_eC_p^2$ in 0.2 M NaCl. The observed decrease in $D_eC_p^2$ at pH = 4 coincides with the pK_a of PVI.[8] As the PVI is deprotonated the repulsive forces within the network are decreased and the mobility of chain segments that apparently controls electron transport diminishes. The pH dependence of D_e was similar to that observed in the POs-EA-peg 400 system[3,9] where charging of the network and absence of screening also facilitated electron transfer. In PVI_n-Os networks swelling at low pH should decrease C_p. Nevertheless, the increase in De was so large that $D_eC_p^2$ still increased.

Permeability of PVI_n-Os-Peg 400 Hydrogels. Permeability of the hydrogels to water soluble substrates and products is important in biosensor applications. For the analysis of permeability p-benzoquinone was chosen as a model compound, because of its known electrochemistry and its non-ionic nature. The diffusional and kinetic characteristics of benzoquinone partitioning through an electrode film has been analyzed by Saveant et al[10], who measured limiting current densities for rotating disk electrodes and obtained Koutecky-Levich plots for polymer film electrodes. Benzoquinone is reduced at pH = 7 at

~0.2 V negative of the redox potential of PVI_n-$Os^{II/III}$, i.e.. at a potential where benzoquinone can not be catalytically reduced by PVI_n-Os^{II}. The benzoquinone electroreduction current densities were measured as a function of film thickness. The current densities decreased upon increasing film thickness more rapidly than they did in POs-EA films. A cross-linked PVI_3-Os film having 6.6×10^{-8} mol/cm^2 of osmium reached a current density of 1.2 mA/cm^2 per mM benzoquinone, while a POs-EA film with 9.7×10^{-8} mol/cm^2 Os had a current density of 2 mA cm^{-2} per mM benzoquinone.[3] The relatively lesser permeability of PVI_n-Os may be a result of ethyl amine spacer groups in POs-EA films, which may loosen the cross-linked structure.

Steady-State Amperometric Glucose Response of Cross-linked PVI_n-Os Films Containing GOX . The steady-state electrooxidation current was measured at 1000 RPM as a function of the amount of enzyme in the films at 48 mM glucose concentration, well above the K_m of the electrodes (figure 3). In electrodes prepared with a fixed amount of 10 μg PVI_n-Os (n = 3, 5, 10), 11% peg 400 (by weight), and 0.5 μg to 60μg GOX, the current densities did not vary with the osmium content of the polymers. They were highest in electrodes containing 8 μg GOX, corresponding to 39 weight %. In a series of electrodes made with 2% to 22% peg 400, the highest current densities were observed in electrodes made with 11% of the cross-linker.

Glucose Diffusion Through Cross-linked Films. Increasing the rotation rate from 100 RPM to 2500 RPM at 10 mM and 48 mM glucose concentrations did not substantially affect the glucose electrooxidation currents. At 1 mM glucose concentration under a nitrogen atmosphere the current decreased only by 14% when the rotation rate was reduced from 2500 RPM to 100 RPM. As will be discussed later, this was not the case when the solution was O_2 saturated. The absence of greater dependence of current density on rotation rate suggests

that the currents were controlled primarily by a process within the films and not by mass transport to the films at $\geq$ 1 mM glucose concentration. Thus, from the measured 1.2 mA cm^{-2} current density for benzoquinone, and assuming that glucose and benzoquinone permeation rates do not differ greatly, one can conclude that the current density is limited either by the rate of electron transfer to the redox polymer from the enzyme's $FADH_2$ centers, or by electron diffusion through the cross-linked polymer.

O_2 Effects on Glucose Response. The steady-state glucose response is shown in figure 4 for a typical cross-linked electrode (10 μg PVI_3-Os, 8 μg GOX, and 2.5 μg peg 400) under N_2, air, and O_2 at 1000 RPM. Evidently, O_2 competes effectively with PVI_3-Os, in the oxidation of $FADH_2$ centers.

At 48 mM glucose concentration, the glucose electrooxidation current decreased by 45% when the bubbled gas was switched from N_2 to O_2. At 2 mM glucose, the decrease was 76%. Apparently, at high glucose concentrations the O_2 flux is consumed in the outer layer of the film, while a substantial inbound glucose flux survives oxidation by O_2 and penetrates the film. Consistently, the loss in current upon switching the atmosphere from N_2 to O_2 was reduced not only at high glucose concentrations but also when thicker cross-linked films were employed or when the films were heavily loaded with GOX. Furthermore, upon decreasing the O_2 flux through stopping the 1000 RPM rotation of the electrodes, the O_2 associated loss diminished (figure 5). The glucose electrooxidation current at $\geq$ 6 mM glucose concentration was greater when the electrode rotation was stopped because of the decrease in O_2 flux. Below 6 mM glucose the behavior was, however normal; i.e. the currents were higher for the rotating electrode, being dominated by glucose flux.

Dependence of the Glucose Response on Film Thickness. Electrodes with films having 1.1 $X10^{-9}$ mol/cm^2 to 9.7 $X\ 10^{-8}$ mol/cm^2 electroactive osmium

were studied. A plot of the steady-state glucose electrooxidation current at 48 mM as a function of the surface density of the osmium centers is shown in figure 7. The c. .ent density increased with the surface density of osmium sites through a 100-fold range. The trend seen in figure 7 is similar to that observed for POs-EA.[4]

pH and NaCl Concentration Dependence of the Glucose Electrooxidation Currents. The dependence of the current density on pH is shown in figure 8. As in the case of POs-EA[11] the catalytic current peaked at and was nearly independent of pH from pH 7.5 to pH 10, in contrast with the GOX catalyzed oxidation of glucose by O_2, where a narrow pH optimum near 5.5 has been observed. Current was lost irreversibly at pH $\geq$ 10, while below pH 7.5 the changes in current with pH were reversible.

The dependence of the current density on NaCl concentration is shown in Figure 9 for a 10 mM phosphate buffer solution (pH = 7.2). The highest glucose current is observed at 50 mM NaCl with the current density decreasing as the NaCl concentration is increased, dropping to approximately half of its maximum value at 300 mM NaCl.

Selectivity of PVI_n-Os Films in the Presence of Interferants. Glucose sensors are often insufficiently selective when operated at potentials where urate, ascorbate, and acetaminophen are also electrooxidized. The resulting errors can be reduced by membranes that preferentially transport glucose. Examples of such membranes are cellulose acetate[12] and Nafion™ [13]. The effects of interferants can also be reduced by poising the electrodes at more negative potentials, where the rate of interferant electrooxidation is reduced.[14] Since the redox potential of PVI_n-Os is cathodic relative to that of POs-EA by 80 mV, the PVI_n-Os electrodes are more selective. When required, glucose selectivity can

be further improved by non-electrochemical catalytic pre-oxidation of the interferants by H_2O_2 in an outer film of horseradish peroxidase.[15]

Figure 10 shows a glucose calibration curve for a thick film electrode (prepared with 560 μg cm^{-2} PVI$_3$-Os, 450 μg cm^{-2} GOX, 140 μg cm^{-2} peg 400) in the absence and presence of 0.1 mM ascorbate. Although in the absence of glucose the ascorbate electrooxidation current was high, this current was small with > 2 mM glucose. The current was increased by the 0.1 mM ascorbate at 6 mM glucose by 9%, corresponding to a +0.5 mM error in the glucose reading. The error was reduced when the glucose concentration was increased. Thus, at 20 mM glucose, the error was only 2%.

Interferants can be electrooxidized at the electrode surface (I_{surf}) and at osmium redox sites (I_{Os}). In electrodes with thin permeable PVI$_3$-Os films interferants were oxidized both directly at the carbon surface and at Os^{III} redox sites, whereas, in thick PVI$_3$-Os films they were oxidized predominantly at the Os^{III} redox sites.

When the glucose electrodes were made with thick PVI$_3$-Os films the ascorbate and acetaminophen caused currents decreased. This reduction in interference is interpreted as resulting from a lesser flux of ascorbate to the carbon surface i.e. from a reduction in I_{surf}. In the bulk of the polymer, where there is competition between ascorbate and $FADH_2$ for Os^{III} sites, I_{Os} decreases upon increasing the glucose concentration. At 0 mM glucose, the concentration of Os^{III} sites is the highest and I_{Os} is largest. Upon increasing the glucose concentration, the $FADH_2$ centers compete with ascorbate for the Os^{III} redox centers and I_{Os} decreases. Note that if ascorbate rather than a $FADH_2$ center is oxidized by an Os^{III} center, then the glucose electrooxidation current (I_G) is decreased, and the increase in I_{Os} is offset by the decrease in I_G.

In thin film electrodes the situation is quite different. A glucose response curve is shown in figure 11 for an electrode with such a thin film (140 μg cm^{-2} PVI_3-Os, 110 μg cm^{-2} GOX, 35 μg cm^{-2} peg 400) in the absence and in the presence of 0.1 mM ascorbate. The ascorbate-related current increment is large, causing a 100% error at 6 mM glucose. The error slightly decreases, however, at high glucose concentration. Evidently, in thin film electrodes I_{surf} is large at high convection. The oxidation of ascorbate is strongly rotation rate dependent, in contrast with the glucose electrooxidation rate, that is nearly independent of the rotation rate.

Thick film PVI_n-Os based glucose electrodes were also selective against acetaminophen. The glucose response curve with 1 mM acetaminophen was similar to that shown for 0.1 mM ascorbate. The addition of urate caused, however, an initial increase in oxidation current, followed by a rapid decay in current output, showing that an intermediate in the electrooxidation of urate damaged at least one group of centers involved in relaying electrons from glucose to the electrode. Cyclic voltammetry confirmed urate electrooxidation by Os^{III} sites and a resulting loss in the surface density of these sites.

Conclusions

The polyvinylimidazole derived redox polymers PVI_n-Os form with GOX, upon cross-linking with a water-soluble diepoxide, hydrogels that are permeable to glucose and through which electrons diffuse. The polymer is simpler and easier to make than the earlier reported polyvinyl pyridine derived POs-EA, and does not require modification with primary amines for cross-linking with the diepoxide at ambient temperature in an aqueous solution. Electrons diffuse through the gel through a chain flexing dependent mechanism, i.e. the rate of

electron diffusion is not controlled by hopping between neighboring redox sites within chains, but by collisions between segments of redox polymer chains. Amperometric glucose sensors made with thick PVI_n-Os and GOX based gels are reasonably selective in their glucose response in the presence of the electroxidizable interferants ascorbate and acetaminophen.

Acknowledgement

We acknowledge support of this work by the Office of Naval Research, The National Science Foundation, The National Institute of Health, and the Robert A. Welch Foundation. We especially thank Ioanis Katakis and Dr. Nigel Surridge for their insightful discussions.

Table I. Effects of the extent of cross-linking and redox site density on $D_eC_p^2$.

Figure 1. Dependence of $D_eC_p^2$ on the concentration of NaCl for electrodes coated with cross-linked PVI_{10}-Os film with 9.1% peg 400.

Figure 2. Dependence of $D_eC_p^2$ on the pH for an electrodes coated with PVI_{10}-Os with 9.1% peg 400.

Figure 3. Dependence of the limiting catalytic current density on the GOX weight fraction for PVI_n-Os [n = 3 (circles), 5 (squares), 10 (triangles)] cross-linked with 11% peg 400. 1000 RPM, 20 mM, pH 7.2, air.

Figure 4. Dependence of the steady-state current density on the glucose concentration for the same electrode under N_2 (circles), air (triangles), and O_2 (squares). Electrode coated with 10 μg PVI_3-Os, 8 μg GOX, and 2.5 μg peg 400. At 1000 RPM

Figure 5. Dependence of the steady-state current density on the glucose concentration under N_2 (circles), air (triangles), and O_2 (squares). Electrode coated as in figure 4. Stagnant solution (no rotation).

Figure 6. Dependence of the steady-state current density on the glucose concentration under O_2 at 1000 RPM (squares) and under stagnant conditions (circles). Electrode coated as in figure 4.

Figure 7. Dependence of the limiting catalytic current density on the surface density of electroactive osmium sites. Conditions as in figure 3 with 48 mM glucose.

Figure 8. Dependence of the steady-state current density on pH. Conditions as in figure 3.

Figure 9. Dependence of the steady-state current density on NaCl concentration. Conditions as in figure 3.

Figure 10. Dependence of the steady-state current density on glucose concentration in the presence of 0.1 mM ascorbate (squares) and without ascorbate (circles). Electrode coated with 40 μg PVI_3-Os, 32 μg GOX, and 10 μg peg 400.

Figure 11. Dependence of the steady-state current density on glucose concentration in the presence of 0.1 mM ascorbate (squares) and without ascorbate (circles). Electrode coated with 10 μg PVI_3-Os, 8 μg GOX, and 2.5 μg peg 400.

[1]Heller, A. J. Phys. Chem. **1992**, 96, 3423-3428

[2]Pishko, M. V.; Michael, A. C.; Heller, A. Anal. Chem. **1991**, 63, 2268-2272

[3]Gregg, B. A.; Heller, A. J. Phys. Chem. **1991**, 95, 5970-5975

[4]Gregg, B. A.; Heller, A. J. Phys. Chem. **1991**, 95, 5976-5980

[5]Lay, P. A.; Sargeson, A. M.; Taube, H. Inorg. Syn. **1986,** 24, 291-299

[6]Forster, R. J.; Vos, J.G. Macromelecules **1990**, 23, 4372-4377

[7]Murray, R. W. In Electroanalytical Chemistry; Bard, A. J., Ed; Marcel Dekker: New York, 1984: pp 191-368

[8]Tan, J. S.; Sochor, A. R. Polym. Prepr. **1979**, 20, 15-18

[9]Aoki, A.; Heller, A. unpublished results

[10](a) Andrieux C.P.; Haas, O.; Saveant J. M. J. Am. Chem. Soc. **1986**, 108, 8175-8182

(b) Andrieux C.P.; Saveant J. M. J. Electroanal. Chem. **1982**, 134, 163-166

(c) Andrieux C.P.; Saveant J. M. J. Electroanal. Chem. **1982**, 131, 1-35

(d) Andrieux C.P.; Dumas-Bouchiat, J. M.; Saveant J. M. J. Electroanal. Chem. **1984**, 169, 9-21

(e) Ledy, J.; Bard, A. J.; Maloy, J. T.; Saveant, J. M. J. Electroanal. Chem. **1985**, 187, 205-227

[11]Katakis, I.; Heller, A. Anal. Chem. 1992, 64,1008-1013

[12]Lobel,E.; Rishpon, J. Anal. Chem. **1981**, 53, 51-53

[13]Bindra, D.S.; Wilson, G.S. Anal. Chem. **1989**, 61, 2566-2570

[14]Cass, A. E. G.; Davis, G.; Francis, G. D.; Hill, H. A. O.; Aston, W. J.; Higgins, I. J.; Plotkin, E. V.; Scott, D. L.; Turner, A. P. F.; Anal. Chem. **1984**, 56, 667-671

[15]Maidan, R.; Heller, A. Anal. Chem. **1992,** 64, 2889-2896

Table I

	$D_eC_p^2$ (X 10^{16} mol^2 cm^{-4} s^{-1})		
%peg 400	PVI_3-Os	PVI_5-Os	PVI_{10}-Os
20.0	18.7	15.3	1.21
16.7	26.6	7.65	3.46
9.1	38.2	11.3	9.92
4.8	36.0	5.60	3.51
Avg $D_eC_p^2$	30.0 ± 9.0	9.96 ± 4.27	4.52 ± 3.7

	D_e (X 10^8 cm^2 s^{-1})*		
%peg 400	PVI_3-Os	PVI_5-Os	PVI_{10}-Os
20.0	0.85	2.34	0.11
16.7	1.29	0.86	0.25
9.1	1.46	1.55	0.68
4.8	2.28	0.57	0.68
Avg D_e	1.47 ± 0.60	1.33 ±0.79	0.43 ± 0.29

Figure1

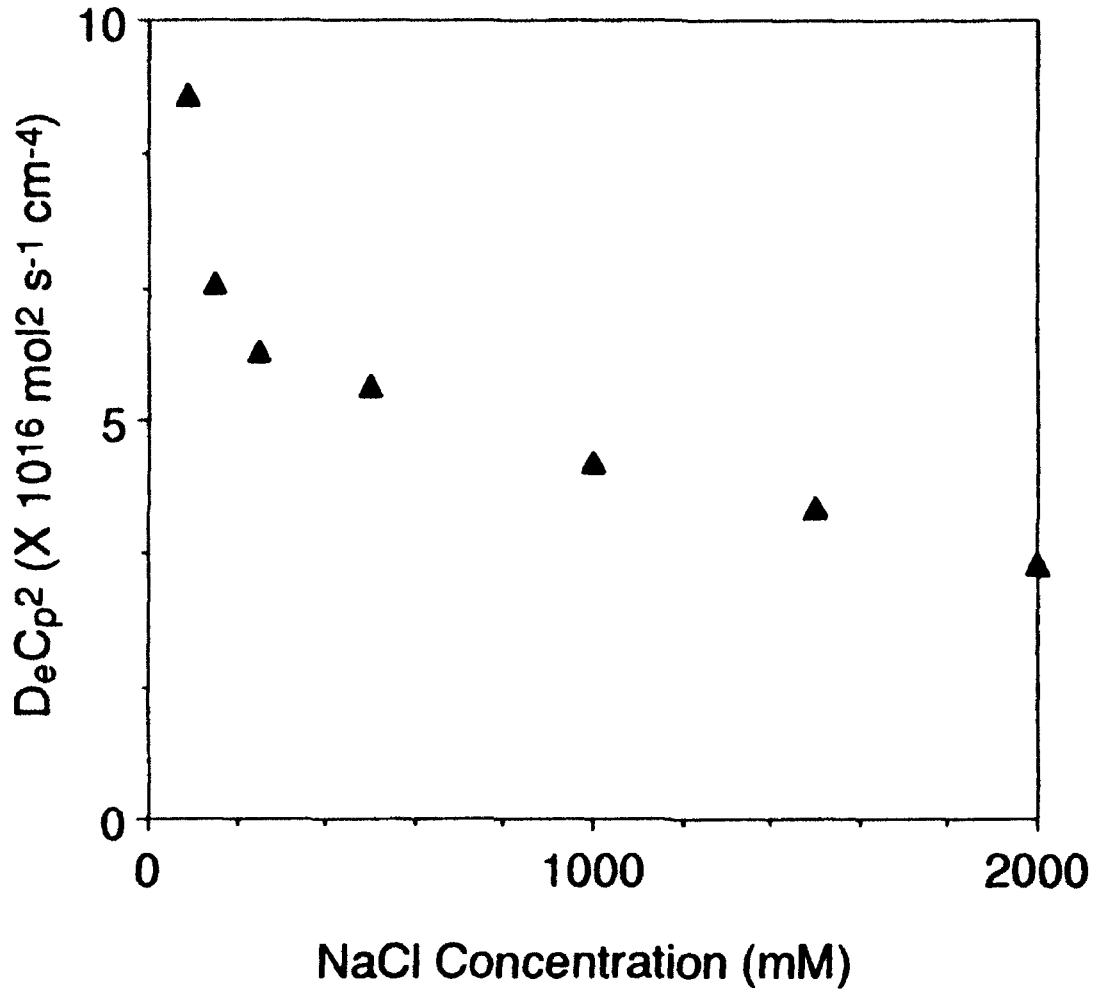
10
5
0
0
1000
2000
$D_eC_p^2$ (X 10^{16} mol^2 s^{-1} cm^{-4})
NaCl Concentration (mM)

Figure 2

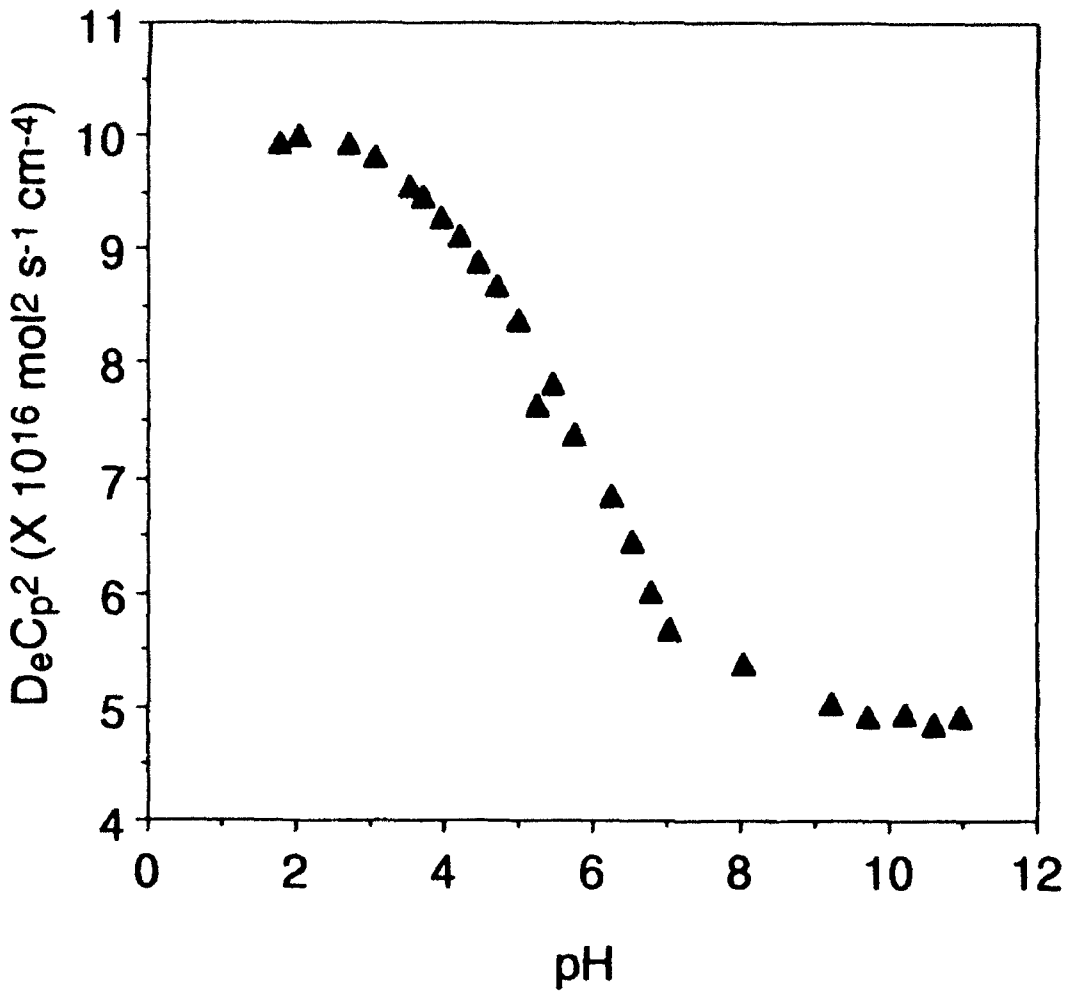

Figure 3

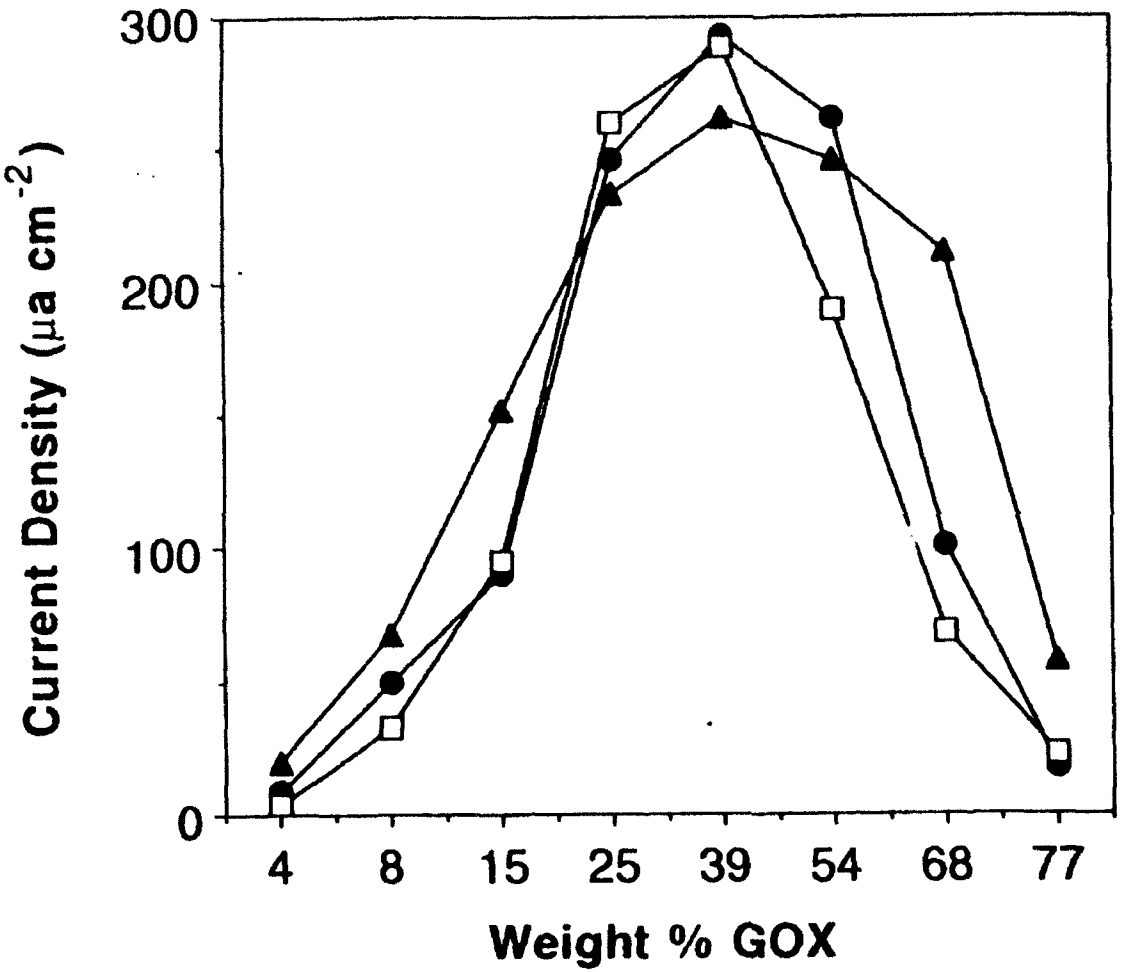
300
200
100
0
Current Density (μa cm-2)
4
8
15
25
39
54
68
77
Weight % GOX

Figure 4

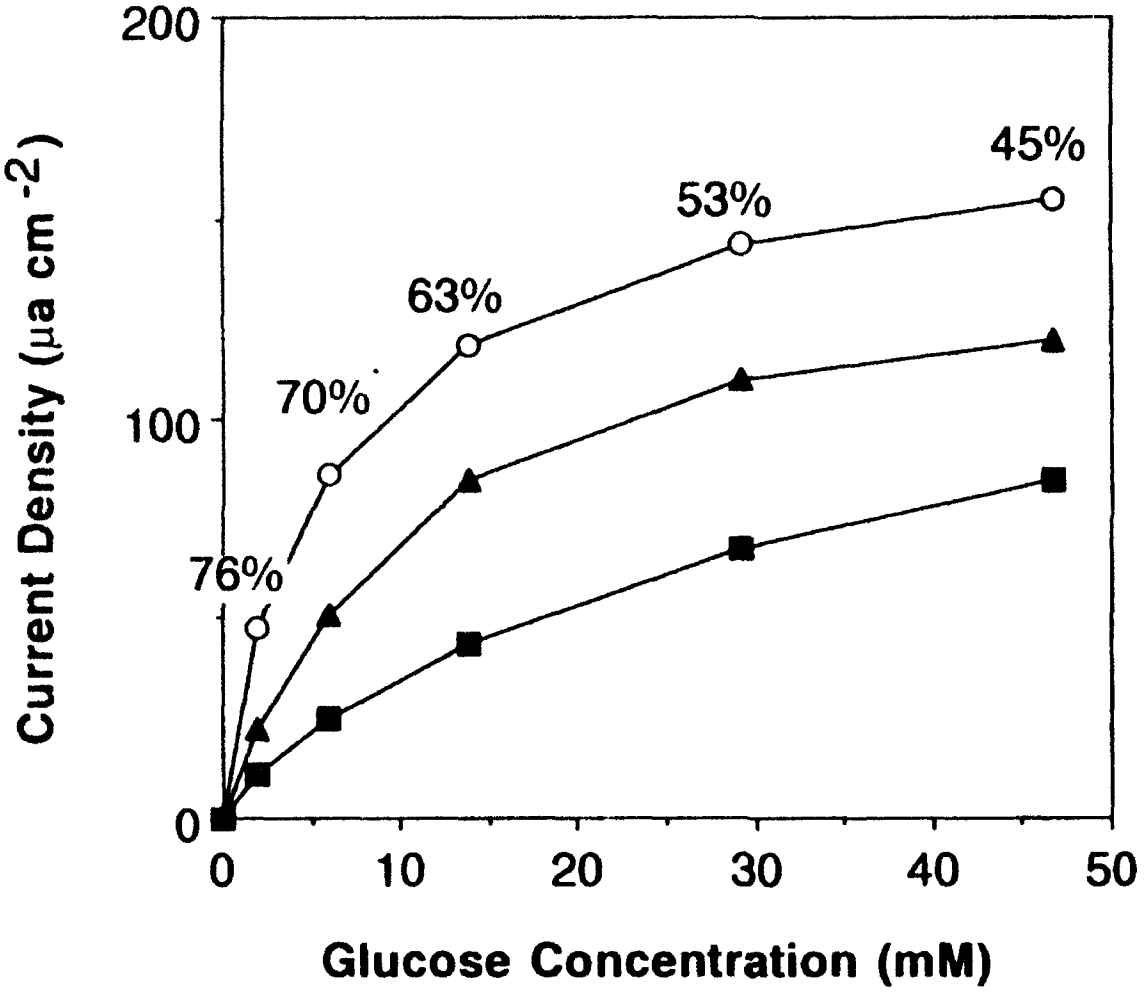
200
100
0
0
10
20
30
40
50
Current Density (μa cm -2)
Glucose Concentration (mM)
45%
53%
63%
70%
76%

Figure #5

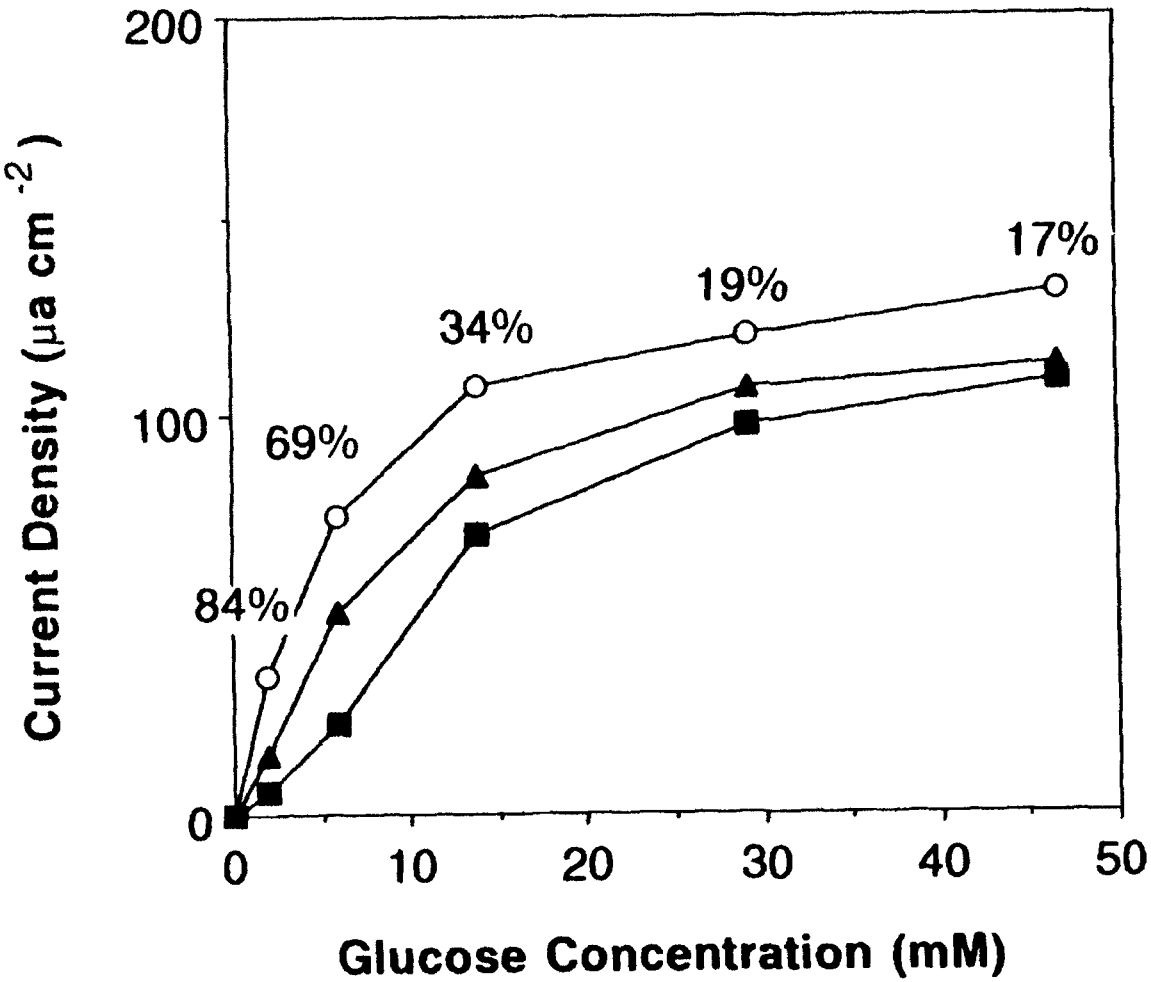
200
100
0
Current Density (μa cm -2)
0
10
20
30
40
50
Glucose Concentration (mM)
17%
19%
34%
69%
84%

Figure 6

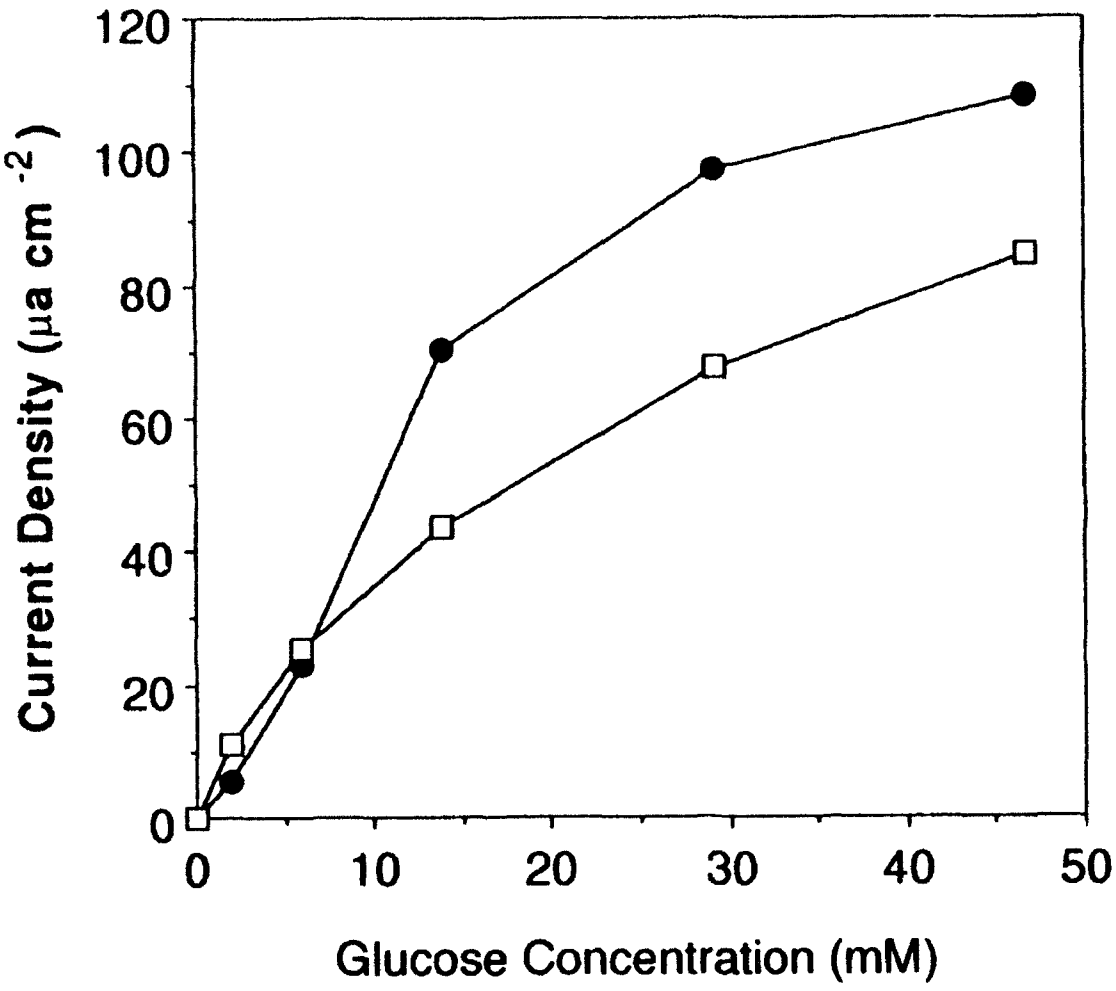
Current Density (μa cm -2)
120
100
80
60
40
20
0
0
10
20
30
40
50
Glucose Concentration (mM)

Figure 7

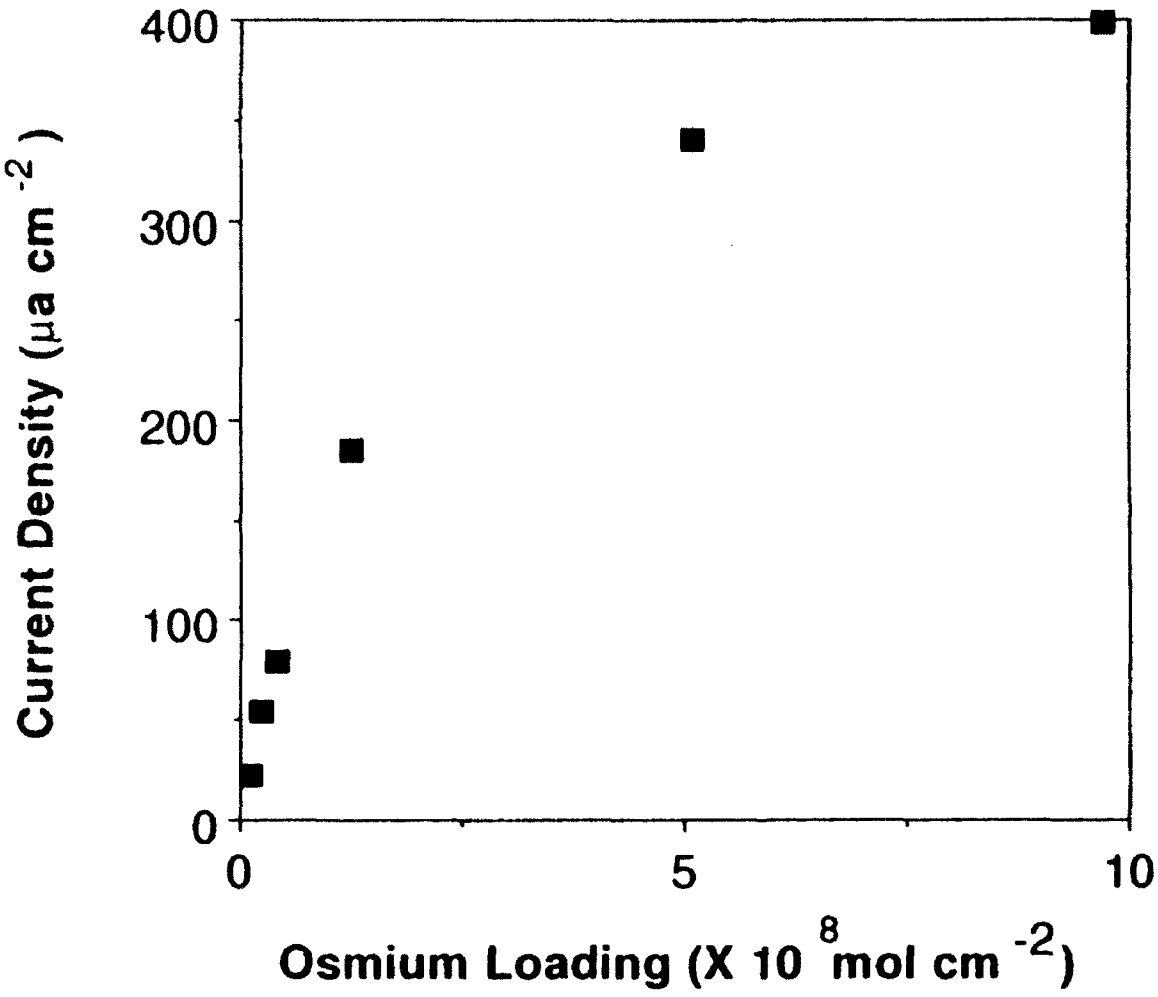
400
300
200
100
0
0
5
10
Current Density (μa cm -2)
Osmium Loading (X 10 8 mol cm -2)

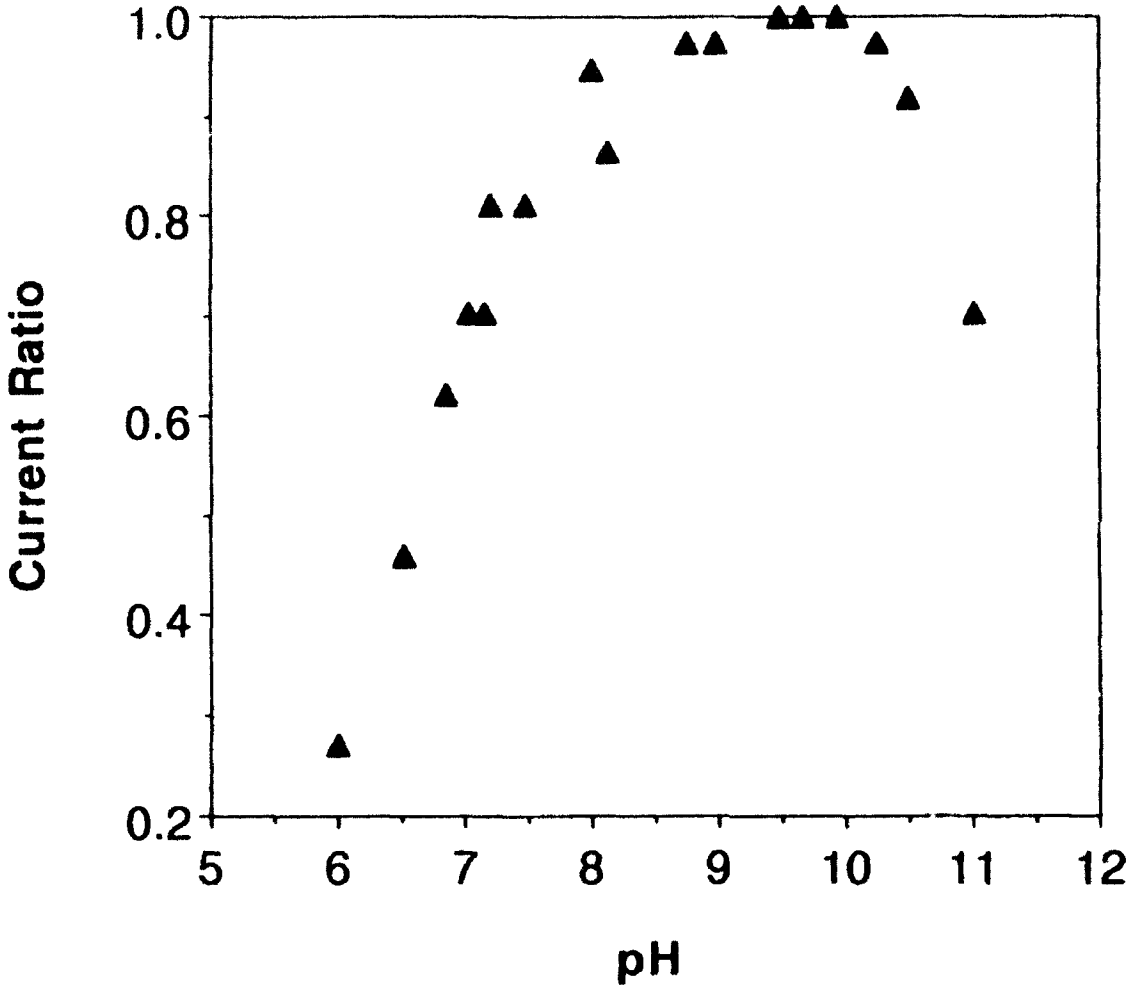
Current Ratio
1.0
0.8
0.6
0.4
0.2
5
6
7
8
9
10
11
12
pH

Figure 9

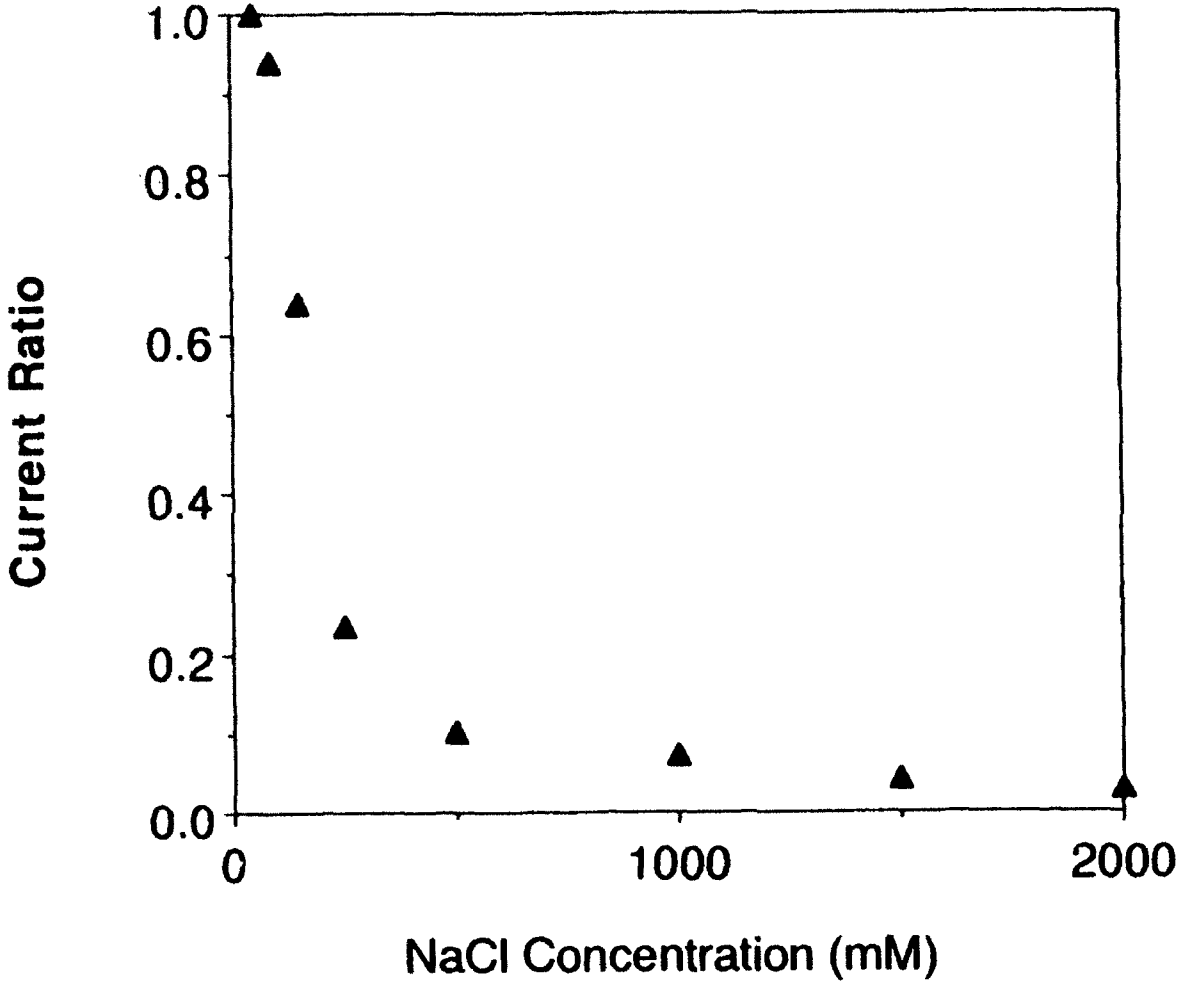
1.0
0.8
0.6
0.4
0.2
0.0
Current Ratio
0
1000
2000
NaCl Concentration (mM)

Figure 10

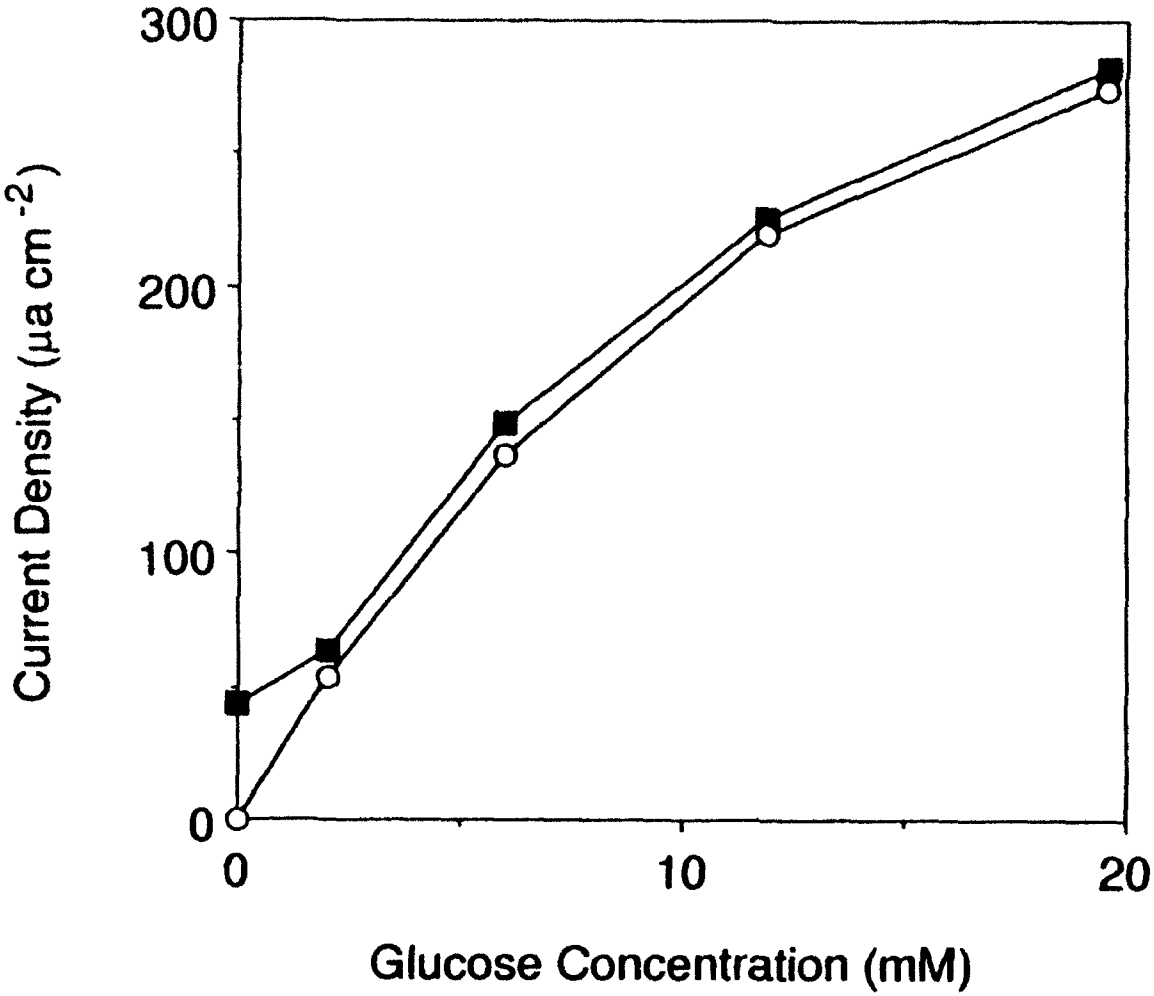
300
200
100
0
0
10
20
Current Density (µa cm -2)
Glucose Concentration (mM)

Figure 11

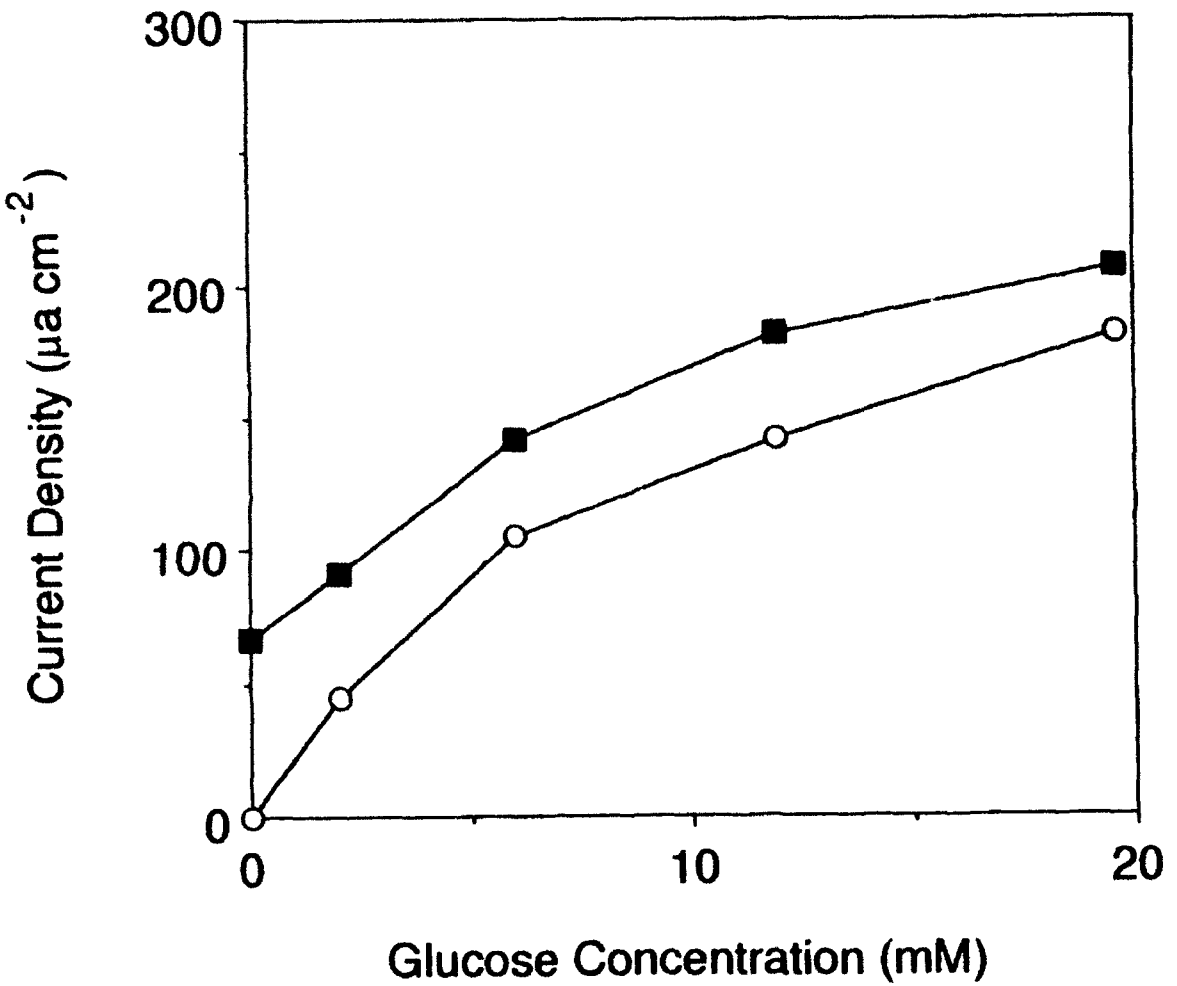
300
200
100
0
0
10
20
Current Density (μa cm-2)
Glucose Concentration (mM)